

CORRECTING THE POLARIZATION LEAKAGE PHASES AND AMPLITUDES THROUGHOUT THE PRIMARY BEAM OF AN INTERFEROMETER

R. I. REID¹, A. D. GRAY, T. L. LANDECKER, AND A. G. WILLIS

Dominion Radio Astrophysical Observatory, Herzberg Institute of Astrophysics, National Research Council, P.O. Box 248,
 Penticton, BC, Canada, V2A 6J9.

To appear in Radio Science.

ABSTRACT

Polarimetric observations are affected by leakage of unpolarized light into the polarization channels, in a way that varies with the angular position of the source relative to the optical axis. The off-axis part of the leakage is often corrected by subtracting from each polarization image the product of the unpolarized map and a leakage map, but it is seldom realized that heterogeneities in the array shift the loci of the leaked radiation in a baseline-dependent fashion. We present here a method to measure and remove the wide-field polarization leakage of a heterogeneous array. The process also maps the complex voltage patterns of each antenna, which can be used to correct all Stokes parameters for imaging errors due to the primary beams.

Subject headings: instrumentation: interferometers — instrumentation: polarimeters — techniques: interferometric — techniques: polarimetric

1. INTRODUCTION

The hardware typically used in radio telescopes has the great benefit of observing the Stokes Q , U , and V parameters simultaneously with Stokes I , but always allows some mixing between the polarization channels, as in Figs. 1 and 2. This “leakage” is particularly troublesome when it goes from I into Q , U , or V , since the polarized signals are usually a small fraction of the total intensity, and therefore easily swamped by similarly strong leakages from I .

A radio interferometer uses two or more antennas to measure the amplitudes and phases of the electric field impinging on their receivers. The measurements are stored as “visibilities”, which are the correlations of the receiver voltages. Given some conditions which this article will assume to have been met, the visibilities sample the Fourier transform of the sky multiplied by the primary beam (directional sensitivity function) of the antennas (Clark 1999; Thompson 1999).

Mathematically, the effect of a pair of antennas A and B on the visibilities they observe, $V_{\text{obs},AB}$, is conveniently expressed using the Hamaker-Bregman-Sault (Hamaker et al. 1996) formalism, where the four polarizations are combined into a column vector. The true visibilities are multiplied on the left by a set of Jones matrices, each one the outer product of Jones matrices for antennas A and B , i.e.

$$D_{AB} = D_A \otimes D_B^*$$

represents the on-axis mixing between the nominally orthogonal polarization channels, often called the “ D terms”. The outer product of two matrices M and N , $M \otimes N$, is formed by multiplying each entry of M with all of N , and is used, along with a complex conjugation of the second factor, to bring together the elements from each antenna in a correlation. Hamaker et al. (1996) explain the algebraic properties, including coordinate transformations, of Jones matrices and the outer product in more detail. As in Bhatnagar et al. (2006), direction dependent effects can also be included, but

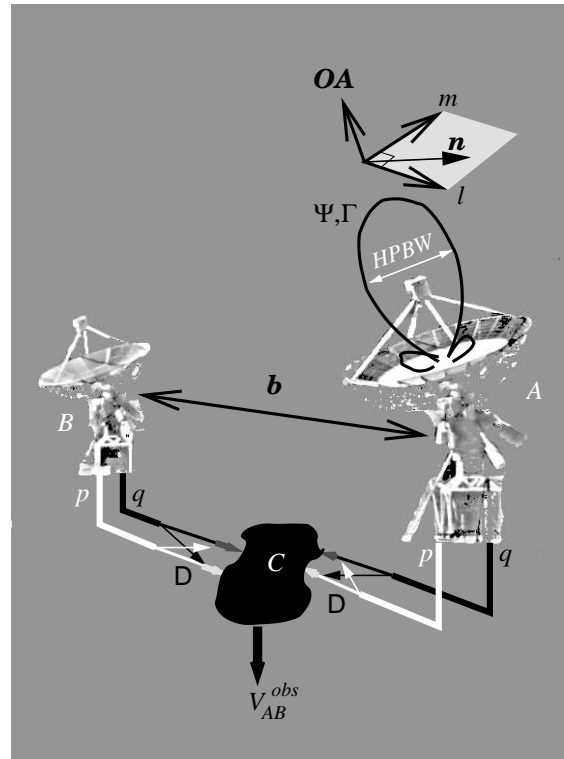


FIG. 1.— Conceptual diagram of polarization leakage in an interferometer. Each antenna measures two nominally orthogonal polarizations p and q , but they are partially mixed before entering the correlator C .

b : Baseline (separation) between antennas.

OA : The optical axis (i.e. pointing direction).

(l, m) : Longitudinal and latitudinal offsets perpendicular to OA .

n : An arbitrary offset in (l, m) .

Γ_A : Voltage pattern of antenna A , factored to exclude polarization leakage.

HPBW: Half Power Beam Width.

D_B : n independent factor of the polarization leakage of antenna B .

Ψ : n dependent factor of the polarization leakage.

$V_{\text{obs},AB}$: Observed vector of visibilities in each polarization.

Although the diagram places Ψ and Γ above the receiver and D below, each includes effects from the feed, reflector surface, and receiver support struts.

Electronic address: rreid@nrao.edu

¹ Now at the National Radio Astrophysical Observatory, 520 Edgemont Rd., Charlottesville, VA, 22903, USA

they must go *inside* the Fourier integral:

$$V_{AB}^{\text{obs}} = D_{AB} \int \Psi_{AB}(\mathbf{n}) \Gamma_{AB}(\mathbf{n}) S I_S(\mathbf{n} + \mathbf{n}_c) e^{i\mathbf{n} \cdot \mathbf{b}_{AB}} d\mathbf{n} \quad (1)$$

where \mathbf{n} is a direction on the sky relative to the “phase tracking center”, \mathbf{n}_c . \mathbf{n}_c is set electronically, but usually it is chosen to coincide with the pointing direction of the antennas. S is the Stokes matrix, which transforms the sky’s Stokes parameters, $I_S = (I, Q, U, V)$, into the observational polarization basis, typically correlations of either circular or linear polarizations. Ψ_{AB} and Γ_{AB} are respectively the wide-field leakage pattern and primary beam for the correlation of antennas A and B . They are sometimes multiplied together to form a single Jones matrix which is a generalization of the primary beam, but the magnitudes of the effects are more easily assessed if they are kept separate. With the separation, Γ_{AB} is diagonal since it does not mix polarizations in the observational basis, and the diagonal elements of Ψ_{AB} are all one.

The on-axis portion of the leakage, D_{AB} , is dealt with by standard polarimetric calibration techniques, but the leakage varies with direction, growing worse toward the edges of the primary beam, as in Fig. 2. This paper is concerned with the wide-field polarization leakage, Ψ_{AB} , and will assume that $V_{\text{obs},AB}$ has already been corrected by multiplication with D_{AB}^{-1} .

If all of the antennas in an array are identical, the effects of the primary beam and leakage patterns can be removed in the image plane. At the Dominion Radio Astrophysical Observatory (DRAO) we previously corrected the wide-field contamination or polarization by multiplying the Stokes I image with “leakage maps”, and subtracting the results from the measured Q and U images, as in Fig. 4. The leakage maps were measured by observing the apparent Q/I and U/I of an intrinsically unpolarized source in a grid of offsets from the primary beam center (Peracaula 1999). This correction is performed completely in the image plane, so we call it the “image-based” leakage removal method. It was immediately applicable for DRAO’s Synthesis Telescope (ST, Landecker et al. (2000)) since its antennas are equatorially mounted and thus its leakage patterns never rotate relative to the sky. The leakage patterns of an altitude-azimuth mounted telescope such as the Very Large Array (VLA) rotate relative to the sky over the course of an observation, but the image-based method can still be applied if the data are first broken up into a series of snapshots (Cotton 1994).

Unfortunately, there are differences, known or unknown, between the antennas of any real interferometer. The array may be a combination of antennas from originally separate telescopes, such as the Combined Array for Research in Millimeter-Wave Astronomy (CARMA, Bock (2006)), and most very long baseline interferometers. It could also be in a transition period where only some antennas have been modified, like the partially Enhanced Very Large Array, and/or have serious surface errors as at (sub)mm wavelengths. The ST is an example of an array where the antennas are similar to each other, but with known differences between them. The two outermost antennas have 9.14 m diameters with four metal struts supporting their receivers, while the other five are 8.53 m in diameter with three struts, made of either metal or fiberglass. The differences in antenna diameter obviously create differences in the half-power beamwidths (HPBW), which at 1420 MHz are 101.8’ for the two outer antennas and 108.8’ for the rest. The variation in the number and composition of the struts affects the scattering of incoming

light, which is an important component of polarization leakage (most of the rest comes from the feeds).

In polarization images the differences between antennas are seen as mismatches between the standard point spread function (PSF, or “dirty beam”) and the PSF of the leakage. When there are phase differences between the leakages of the antennas, the effective PSF of the leakage is asymmetric (Ekers 1999) and offset from the peak of the unpolarized emission. The effective PSF of the leakage also varies across the field, meaning that subtracting a multiplication of the Stokes I map with a leakage map cannot fully correct the polarization leakage of a heterogeneous array. Additionally, the response of each antenna in an array, both in leaked and true radiation, depends on the scale of the source(s). Resolved features have less power at high spatial frequencies, so antennas that only participate in long baselines will contribute little leakage to them. Unresolved features have no such attenuation with baseline length, and elicit an equally weighted mix of leakage from all antennas. Usually leakage maps are measured using a bright unresolved object, so in the case of a heterogeneous array their corrections are only accurate for unresolved sources.² Fig. 4 exhibits both of these problems, as can be seen in comparison with Fig. 5, the same image corrected with the method described in Section 2. The main change for the unresolved sources is the presence or lack of surrounding arcs, but the supernova remnant also shows a strong difference in the on-source residual leakage.

The work described here aims to improve polarization imaging from the DRAO ST. The telescope is engaged in an extensive survey of the major constituents of the Interstellar Medium, the Canadian Galactic Plane Survey (CGPS, Taylor et al. (2003)) which includes imaging in Stokes parameters Q and U at 1420 MHz along the plane of the Milky Way.

We recently measured the real and imaginary parts of the leakage patterns for each antenna of the ST (similar to a hologram measurement, but with finer spacing over a smaller area) and have started using them to correct its Q and U observations, as seen in Fig. 5.

2. REMOVING LEAKAGE FROM LINEAR POLARIZATION FOR A HETEROGENEOUS ARRAY

When the polarization leakage (or primary beam) varies with both direction and baseline (i.e. antenna pair), there is no way to isolate their effects to one of either the image or uv planes. Multiplying $V_{\text{obs},AB}$ on the left by $\Psi_{AB}^{-1}(\mathbf{n})$ does not work as it does for D_{AB} , because \mathbf{n} must be marginalized away by integrating with I_S . I_S is the true intensity distribution of the sky, which is unfortunately unknown. A set of Stokes I CLEAN (Högbom 1974) components makes an acceptable substitute, however, both in the replacement of the true sky by CLEAN components, and the temporary neglect of Q , U , and V .

Since the correction for a heterogeneous array must be added directly to the visibilities, the I model used must match the true I visibility function within the sampled part of the uv plane. Specifically, it should not be tapered by any sort of smoothing in the image plane, and the almost certain discrepancies between the CLEAN components and true visibility function outside the sampled part of the uv plane are immaterial for this purpose. The CLEANed I image should have small enough pixels to avoid quantization errors in the com-

² Even then, only if the images are made with the same baseline weighting as used for the leakage map.

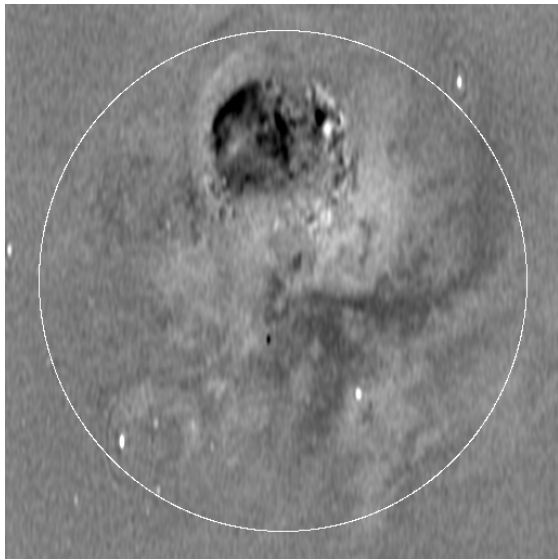


FIG. 2.— An example of leakage from Stokes I into Stokes U in a CGPS field containing the supernova remnant IC443. The thin circle is the $75'$ radius (24% power) cutoff of the usable part of the beam in polarization. The image has not been corrected for the sensitivity dropoff of the primary beam, and only includes ST data. Note that it has been CLEANed, so the arcs are mostly leakage. The grayscale goes from -5 (black) to 5 (white) mJy/beam.

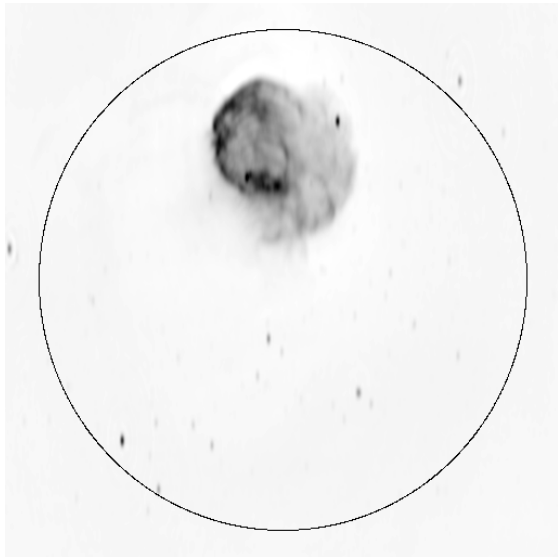


FIG. 3.— The sources of the I radiation that leaked into Fig. 2. The grayscale goes from -12 (white) to 350 (black) mJy/beam.

ponent positions, and be CLEANed to at least a moderately faint level. Very faint I emission does not need to be included since it will be multiplied by the leakage, typically less than a few percent, and it tends to have many more components, which would considerably slow down the calculation of the correction. Leakage from such emission could be quickly and adequately removed by the image-based leakage map method, using the CLEAN residual image as the I map. Calculating the correction for both Q and U of a CGPS field, with a variable number, on the order of several thousand, of CLEAN components, and 1.2×10^5 visibilities per polarization, takes from 15 minutes to overnight on a 2 GHz personal computer.

Assuming that $I_s = (I, 0, 0, 0)$ in correcting the wide-field

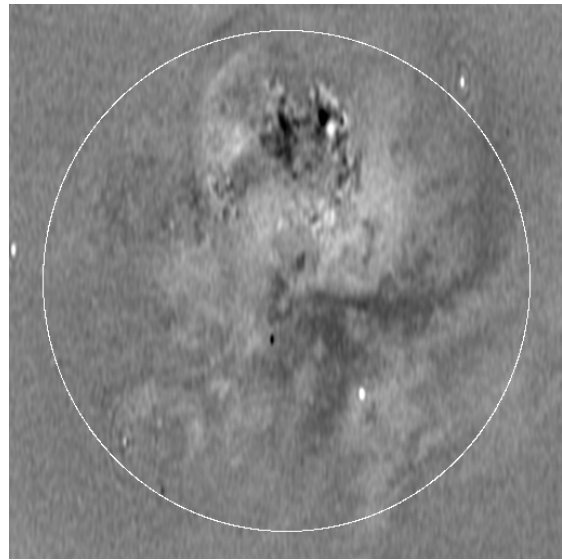


FIG. 4.— Fig. 2 (same grayscale) after image-based leakage correction. The “on-source” correction of unresolved sources is accurate to 1% of I , close to the theoretical precision of the measured leakage map, but the arcs around strong leakage remain unaffected. Leakage amplitude differences between antennas produce rings, and phase differences produce asymmetric arcs.

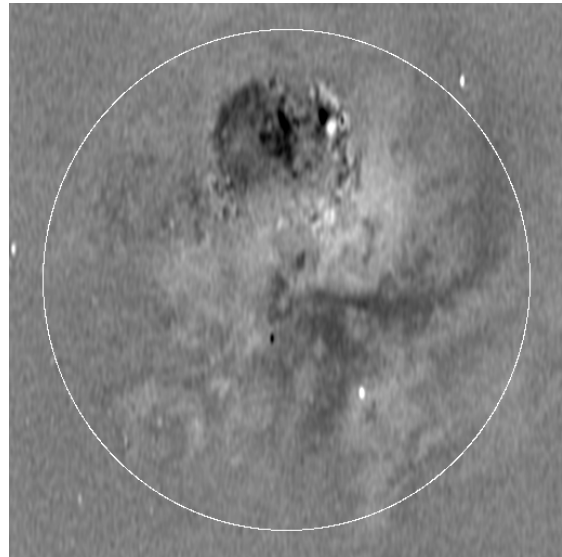


FIG. 5.— Fig. 2 (same grayscale) after correcting leakage using measured patterns for each antenna. Leakage measurements were made only inside the circle, but they have been extrapolated to the edge of the image, which works well for clearing up the arcs of sources slightly outside the limit. The remaining arcs are primarily due to differences between the primary voltage patterns of the antennas.

leakage of Eq. 1 requires some care, since its validity depends on what Stokes parameters are wanted, and whether the feeds are circularly or linearly polarized. In general each measured Stokes parameter is nominally the true Stokes parameter, plus first order leakage from two of the other Stokes parameters, plus second order leakage from the remaining one. This comes from the leakage Jones matrices for each antenna having only ones on diagonal, with the leakage terms off-diagonal. As a rule of thumb, the true Q and U can be thought of as fractions of I , and V as an even smaller fraction (i.e. second order). With circularly polarized feeds the leakage of I into V is second order, and thus possibly of the same magnitude as the leakage from linear polarization, but

the fact that $V = (RR - LL)/2$ means it is more likely corrupted by errors in the right and left gains. Linearly polarized feeds replace V with one of Q or U in a similar situation. If necessary, multiple Stokes parameters can be CLEANed to form an estimate of I_S , to be iteratively improved using the procedure below.

The visibilities are corrected using the set of I_S CLEAN components V_C by subtracting

$$\mathcal{L}b_{AB}(t) = \sum_j \Psi_{AB}(\mathbf{n}_j) V_{C,b_{AB}(t),j} \quad (2)$$

from the visibilities in each polarization at baseline $b_{AB}(t)$. $V_{C,b_{AB}(t),j}$ is the set of visibilities in each polarization for antennas A and B at time t for the j th CLEAN component. We prefer to use $V_{C,b_{AB}(t),j}$ in the form of Stokes parameters instead of feed correlations since usually only one image (I) needs to be CLEANed before applying the correction. Ψ_{AB} is therefore transformed into Stokes form, $\Psi_{S,AB}$:

$$\Psi_{S,AB} = \mathbf{S}^{-1} \Psi_{AB} \mathbf{S}. \quad (3)$$

For the ST, with its circularly polarized feeds, the correction is only applied to Stokes Q and U and second order leakages are ignored since the leakage from I to Q and U is first order. That reduces the used portion of $\Psi_{S,AB}$ to linear combinations of elements of Ψ_A and Ψ_B^* , allowing the leakages of I into Q or U for a given baseline to be easily calculated on the fly from combinations of leakage maps for the individual antennas instead of storing leakage maps for each combination of antennas:

$$l_{PAB} = l_{PA} + l_{PB}^* \quad (4)$$

where P is Q or U . Note that the imaginary part would be cancelled out if A and B were identical. The Jones matrices of individual antennas are in circular coordinates ($p = R, q = L$), so

$$l_{QA} = \Psi_{A,12} - \Psi_{A,21}, \text{ and} \quad (5)$$

$$l_{UA} = -i(\Psi_{A,12} + \Psi_{A,21}). \quad (6)$$

These are the leakage patterns that are shown in Figs. 6 to 9. Note that the 12 and 21 subscripts refer to the off-diagonal elements of the Jones matrix, not baselines between antennas 1 and 2.

3. SIMULATED LEAKAGE MAPS

Ng et al. (2005) calculated theoretical leakage voltage patterns for the ST's three and four metal strut antennas. Applying them to correcting polarization leakage in the CGPS (Taylor et al. 2003) confirmed that heterogeneity in the ST was having a noticeable effect on the CGPS polarization images that was not being corrected by subtracting the Stokes I images multiplied by leakage maps. The correction still left significant residuals, however, which was not surprising since the simulated patterns were based on an overly simplistic model of the ST. Some of the three-strut antennas have fiberglass supports for their receivers. Treating those as zero strut antennas would be incorrect because each receiver box has cables running along one of its supporting struts. The unknown effective blockage of those cables, along with the partial transparency of the fiberglass struts, made measuring the actual leakage patterns essential.

4. ANTENNA PATTERN MEASUREMENTS

If one antenna, A , in an interferometer points directly at a bright isolated source while the others look at it askew, A will not have any off-axis leakage or primary beam attenuation ($\Psi_A(\mathbf{0}) = \Gamma_A(\mathbf{0}) = 1$), and the effective leakage and primary beam patterns will be those of the other antennas alone. Such offset observations with one antenna on axis are often done for hologrammatic measurements of antenna surface errors, and with two modifications the hologram scheme can be adapted to measure the leakage and primary complex voltage patterns of each antenna.

The first modification is to compress the sampling grid of offsets. Since there is a Fourier transform relationship between the physical features of an antenna and its angular power pattern, hologram measurements need to sample a wide section of the celestial sphere to resolve small scale errors (i.e. a misadjusted panel or smaller) on an antenna. In an antenna pattern measurement, however, it is more important to sample the main lobe well, so we confined the sampling grid to within the first null. In theory³ the antenna patterns should not vary any faster with angle than the primary beam. For the ST that means its patterns should be fairly smooth on scales smaller than approximately a degree, so the measurements were made on a grid with 25' spacing out to a maximum distance of 75' from the beam center (the extent of beam used for polarization mosaics).

The second modification is only in software, in that the antenna patterns come directly from the measured visibilities, instead of requiring a Fourier transform like surface error measurements. The primary voltage pattern of an antenna B comes from a observation with an on-axis reference antenna A of an unpolarized and unresolved source s :

$$V_{AB}^{\text{obs}} = (\Psi_A(\mathbf{0}) \otimes \Psi_B^*(\mathbf{n})) (\Gamma_A(\mathbf{0}) \otimes \Gamma_B^*(\mathbf{n})) \mathbf{S} I_S. \quad (7)$$

Since the source is effectively $I\delta(\mathbf{0})$ the integral of Eq. 1 was readily evaluated for Eq. 7. It can be further simplified by noting that $\Psi_A(\mathbf{0})$ and $\Gamma_A(\mathbf{0})$ are identity matrices, and that (unsurprisingly, given the physics it represents) the outer product has the redistribution property (Eq. 5 of Hamaker et al. (1996)):

$$(\mathbf{M}_A \otimes \mathbf{M}_B) (\mathbf{N}_A \otimes \mathbf{N}_B) = (\mathbf{M}_A \mathbf{N}_A) \otimes (\mathbf{M}_B \mathbf{N}_B).$$

Eq. 7 becomes:

$$V_{AB}^{\text{obs}} = \langle v_s \otimes (\Psi_B(\mathbf{n}) \Gamma_B(\mathbf{n}) v_s)^* \rangle \quad (8)$$

$$= \left[\begin{array}{l} \Gamma_{B,11}^*(\mathbf{n}) \langle p_s p_s^* \rangle + \Gamma_{B,22}^*(\mathbf{n}) \Psi_{B,12}^*(\mathbf{n}) \langle p_s q_s^* \rangle \\ -\Gamma_{B,11}^*(\mathbf{n}) \Psi_{B,21}^*(\mathbf{n}) \langle p_s p_s^* \rangle + \Gamma_{B,22}^*(\mathbf{n}) \langle p_s q_s^* \rangle \\ \Gamma_{B,11}^*(\mathbf{n}) \langle q_s p_s^* \rangle + \Gamma_{B,22}^*(\mathbf{n}) \Psi_{B,12}^*(\mathbf{n}) \langle q_s q_s^* \rangle \\ -\Gamma_{B,11}^*(\mathbf{n}) \Psi_{B,21}^*(\mathbf{n}) \langle q_s p_s^* \rangle + \Gamma_{B,22}^*(\mathbf{n}) \langle q_s q_s^* \rangle \end{array} \right]$$

v_s is (p_s, q_s) , the voltages that s nominally imposes on the feeds. s is unpolarized, so $\langle p_s q_s^* \rangle = \langle q_s p_s^* \rangle = 0$, and $\langle p_s p_s^* \rangle = \langle q_s q_s^* \rangle$, reducing Eq. 8 to

$$V_{AB}^{\text{obs}} = \frac{\langle p_s p_s^* \rangle + \langle q_s q_s^* \rangle}{2} \left[\begin{array}{l} \Gamma_{B,11}^*(\mathbf{n}) \\ -\Gamma_{B,11}^*(\mathbf{n}) \Psi_{B,21}^*(\mathbf{n}) \\ \Gamma_{B,22}^*(\mathbf{n}) \Psi_{B,12}^*(\mathbf{n}) \\ \Gamma_{B,22}^*(\mathbf{n}) \end{array} \right].$$

³ Both the simulations of Ng et al. (2005) and the more intuitive realization that objects smaller than the antenna diameter, such as struts, produce features broader than the primary beam.

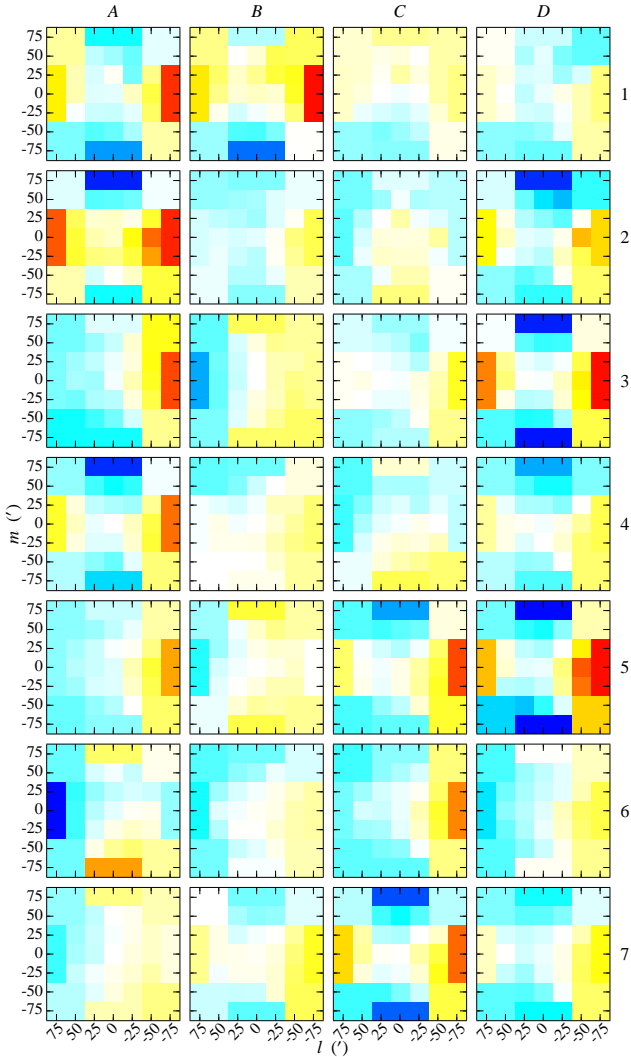


FIG. 6.— Real parts of the voltage leakage from I into Q of antennas 1 (top) to 7 (bottom) for bands A (left) to D (right). The colorscale goes from -0.05 (blue) to 0.05 (red).

The off-diagonal elements of B 's leakage Jones matrix are

$$\Psi_{B,12}(\mathbf{n}) = (V_{AB,qp}^{\text{obs}}/V_{AB,qq}^{\text{obs}})^*, \text{ and}$$

$$\Psi_{B,21}(\mathbf{n}) = (V_{AB,pq}^{\text{obs}}/V_{AB,pp}^{\text{obs}})^*,$$

which completely specifies Ψ_B , since the diagonal elements are 1.

Measuring the primary voltage patterns requires knowing $\langle p_s p_s^* \rangle$ ($= \langle q_s q_s^* \rangle$). Their diagonal entries (the only nonzero ones) can be estimated⁴ from a regular on-axis observation (i.e. $\langle p_A(\mathbf{0}) p_B^*(\mathbf{0}) \rangle$), so

$$\Gamma_{B,11}(\mathbf{n}) \simeq \left(\frac{\langle p_A(\mathbf{0}) p_B^*(\mathbf{n}) \rangle}{\langle p_A(\mathbf{0}) p_B^*(\mathbf{0}) \rangle} \right)^*, \text{ and}$$

$$\Gamma_{B,22}(\mathbf{n}) \simeq \left(\frac{\langle q_A(\mathbf{0}) q_B^*(\mathbf{n}) \rangle}{\langle q_A(\mathbf{0}) q_B^*(\mathbf{0}) \rangle} \right)^*.$$

⁴ To within the noise, since the effects of the primary voltage patterns are defined to be whatever is left after on-axis calibration.

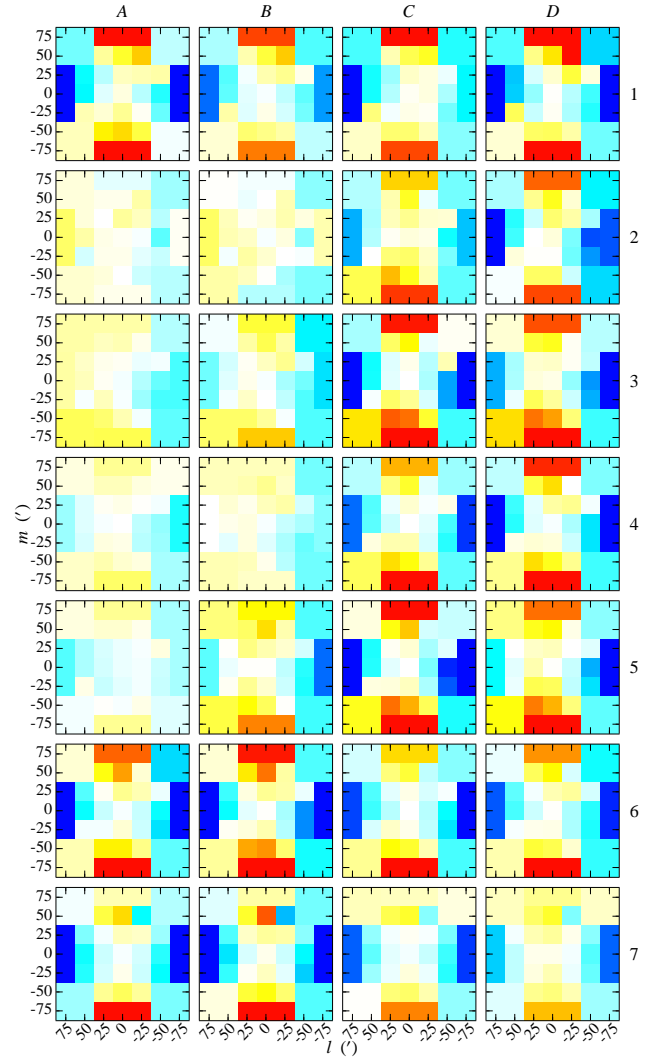


FIG. 7.— Imaginary parts of the voltage leakage from I into Q of antennas 1 (top) to 7 (bottom) for bands A (left) to D (right). The colorscale goes from -0.05 (blue) to 0.05 (red).

The 1420 MHz feeds of the ST are not offset from the central axes of the antennas, so there should be no difference between its $\Gamma_{B,11}(\mathbf{n})$ and $\Gamma_{B,22}(\mathbf{n})$ because of beam squint. We therefore collapse its primary voltage patterns from Jones matrices to a scalar for each antenna:

$$g_{\text{off-axis},B}(\mathbf{n}) \simeq \left[\frac{\langle p_A(\mathbf{0}) p_B^*(\mathbf{n}) \rangle}{\langle p_A(\mathbf{0}) p_B^*(\mathbf{0}) \rangle} + \frac{\langle q_A(\mathbf{0}) q_B^*(\mathbf{n}) \rangle}{\langle q_A(\mathbf{0}) q_B^*(\mathbf{0}) \rangle} \right] / 2.$$

This approach can even be useful for telescopes with offset feeds, such as the VLA, if care is taken to perform all calibration and self-calibration with $I = (pp + qq)/2$ instead of pp and/or qq individually (conversation with J. Uson, 2006). In practice there is some error introduced for wide-field polarimetry by approximating Γ with a scalar, since although Γ does not mix polarizations in the observational basis, it typically does in the Stokes basis. For circularly polarized feeds squint mixes I and V for directions away from the pointing center. This does not greatly contaminate I since V is almost always ~ 0 , but is a serious problem for measuring V , especially for continuum observations where spectroscopic techniques cannot help. The ST does have 1-2% leakage from I into V at the half-power level of the primary beam, and al-

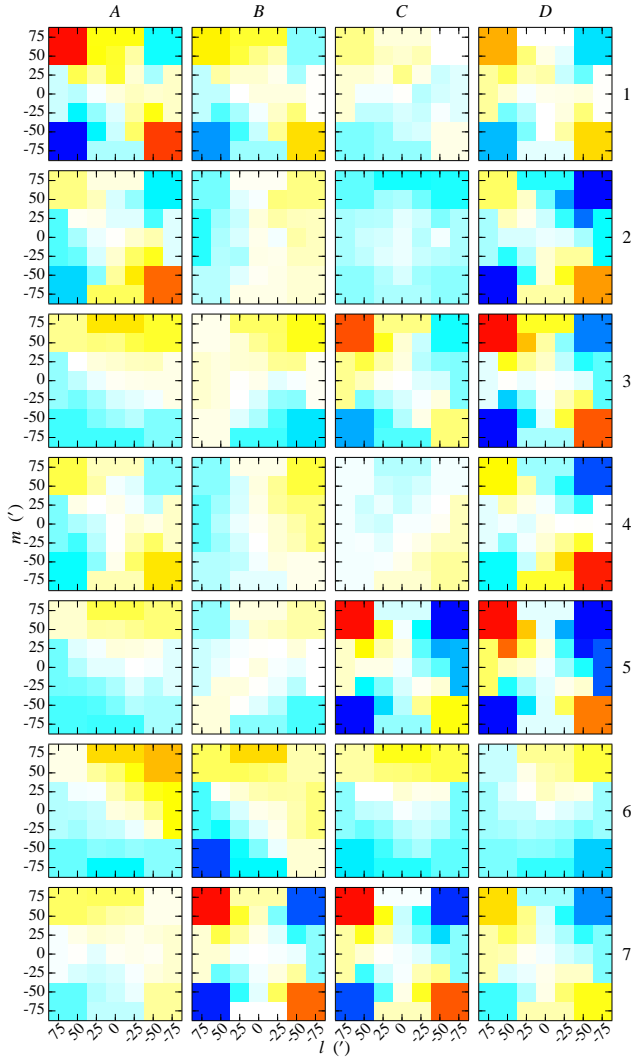


FIG. 8.— Real parts of the voltage leakage from I into U of antennas 1 (top) to 7 (bottom) for bands A (left) to D (right). The colorscale goes from -0.05 (blue) to 0.05 (red).

though it could be interpreted as squint the direction of the apparent squint sweeps through 180° as the frequency goes from band A to D. The Robert Byrd Telescope at Green Bank also sees a change in the direction of the apparent squint with frequency (Heiles et al. 2003). Such a variance with frequency is inconsistent with the geometrical effect that affects the VLA. The ST has only been used to measure V for exceptional cases like pulsars and the Sun, that have strong circular polarization. Observations that need to measure V off-axis for more weakly polarized sources, especially in continuum, will need to apply a more extensive treatment. Similarly, when using linearly polarized feeds (Sault & Ehle 1996) squint mixes I with Q instead of V , making the $\Gamma_{11}(\mathbf{n}) = \Gamma_{22}(\mathbf{n})$ approximation less attractive.

Using g , the primary beam $B_{s,t}(\mathbf{n})$ for a baseline formed by correlating antennas s and t is then

$$B_{s,t}(\mathbf{n}) = g_{\text{off-axis},s}(\mathbf{n})g_{\text{off-axis},t}^*(\mathbf{n}).$$

Note that the order of s and t matters when antennas s and t are not identical.

Since the patterns are ratios, the requirement above that s be unresolved can be loosened to requiring that its size be much smaller than the angular scale of variations in the pri-

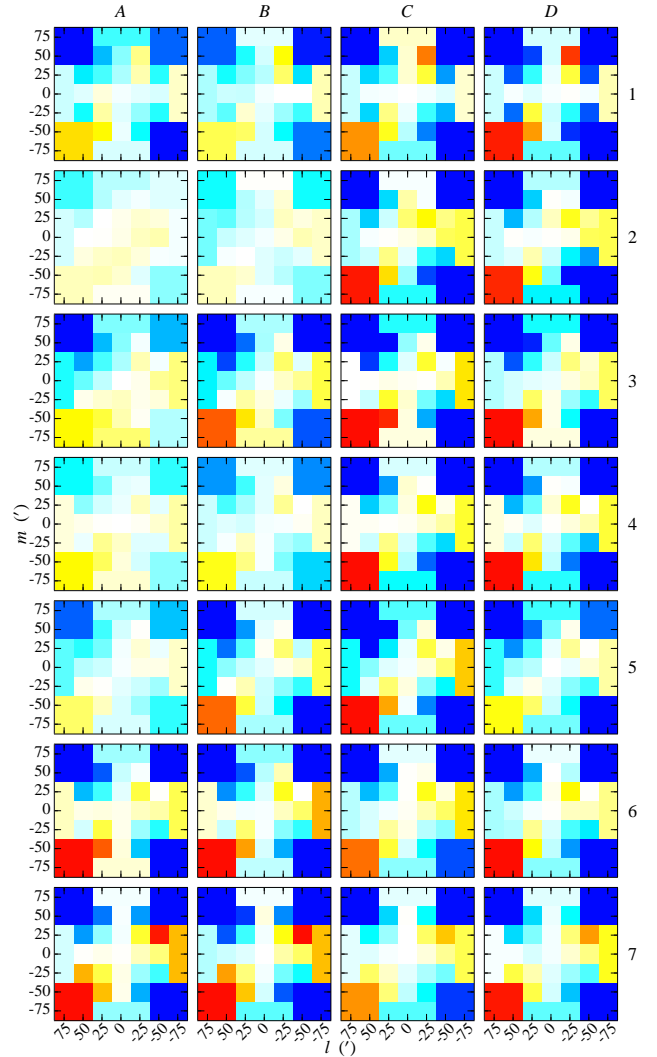


FIG. 9.— Imaginary parts of the voltage leakage from I into U of antennas 1 (top) to 7 (bottom) for bands A (left) to D (right). The colorscale goes from -0.05 (blue) to 0.05 (red).

mary beam, to avoid smearing the pattern samples.

With an interferometric array the patterns can be simultaneously measured for all of the antennas except the reference antenna (i.e. B is anything but A in the above equations) by keeping only the reference antenna pointed at the source while the other antennas look at it with the same grid of offsets. The patterns of the antenna used as a reference in that set of observations can be measured by repeating the observations with a different antenna as the reference.

5. OBSERVED LEAKAGE MAPS

In order to minimize any effects from interference or crosstalk the antennas were placed so that the distances between them were no smaller than 47 m. Observations were made of 3C 147, an unresolved bright source with a flux density of 22 Jy at 1420 MHz.

The beams were sampled on a square grid with $25'$ spacing out to a maximum radius of $75'$ from the beam center. The time spent on each spot was varied to achieve approximately the same uncertainty for each leakage measurement, by making the integration intervals inversely proportional to

the nominal value of the primary beam:

$$t_{\text{int}}(\mathbf{n}) \propto \cos^{-6} \left(\frac{2 \arccos(2^{-1/6})}{\text{HPBW}} |\mathbf{n}| \right). \quad (9)$$

The on-axis pointing was observed longer because it was observationally convenient and it is relatively important since it is used to normalize the patterns.

The entire grid was observed twice, once with antenna 1 as the reference antenna, and then again with antenna 7 as the reference antenna. That allowed the leakage maps and primary voltage patterns of all antennas in the ST to be measured without requiring a separate reference antenna.

The leakage patterns were sampled out to 75' away from the beam center, because that is the portion of the beam used by the CGPS. Beyond that limit (the 24% power level of the beam) the leakages are expected to be large, and require long integration times to measure with the same accuracy. To help remove errors that extend within the 75' from objects just outside it, the leakage pattern measurements are extrapolated, using a nearest-neighbor method, as far as 120' away from the beam center. The leakage patterns are also interpolated with cubic splines to a grid with 0.20' spacing to match the pixels of the CLEAN component images. An example correction with the measured patterns of leakage from I into U is shown in Fig. 5.

6. QUALITY OF LEAKAGE CORRECTION

Since the form of primary beam used in Equation 9 is not necessarily the correct one, the uncertainty in the primary voltage pattern for antenna A , $g_{\text{off-axis},A}(\mathbf{n})$, is calculated as:

$$\left(\frac{\sigma_{g_{\text{off-axis},A}}(\mathbf{n})}{g_{\text{off-axis},A}(\mathbf{n})} \right)^2 = \frac{1}{n_{\text{samps},A}(\mathbf{n})} \left(\frac{\sigma_{I,1\text{samp},A}(\mathbf{n})}{I_A(\mathbf{n})} \right)^2 + \left(\frac{\sigma_{I_A}(\mathbf{0})}{I_A(\mathbf{0})} \right)^2,$$

$$\sigma_{g_{\text{off-axis},A}}(\mathbf{n}) = \left(\frac{n_{\text{samps},A}(\mathbf{0})}{n_{\text{samps},A}(\mathbf{n})} + |g_{\text{off-axis},A}|^2(\mathbf{n}) \right)^{1/2} \frac{\sigma_{I_A}(\mathbf{0})}{I_A(\mathbf{0})}.$$

$g_{\text{off-axis},A}(\mathbf{n})$ gets its name from acting like direction dependent factor of A 's gain. $n_{\text{samps},A}(\mathbf{n})$ is the number of samples for antenna A in direction \mathbf{n} .

$l_{QA}(\mathbf{n})$ is calculated (for an antenna A that comes before the reference antenna, B) as

$$l_{QA}(\mathbf{n}) = \frac{1}{2} \left[\frac{\langle R_A(\mathbf{n})L_B^*(\mathbf{0}) \rangle + \langle L_A(\mathbf{n})R_B^*(\mathbf{0}) \rangle}{\langle L_A(\mathbf{n})L_B^*(\mathbf{0}) \rangle + \langle R_A(\mathbf{n})R_B^*(\mathbf{0}) \rangle} \right]$$

$$= \frac{\langle (R + \Psi_{A,12}L)(\mathbf{n})L(\mathbf{0}) \rangle}{2 \langle L(\mathbf{n})L^*(\mathbf{0}) \rangle} + \frac{\langle (L + \Psi_{A,21}R)(\mathbf{n})R^*(\mathbf{0}) \rangle}{2 \langle R(\mathbf{n})R^*(\mathbf{0}) \rangle}$$

$$= \frac{1}{2} \left[\left(\frac{\langle R(\mathbf{n})L^*(\mathbf{0}) \rangle}{\langle L(\mathbf{n})L^*(\mathbf{0}) \rangle} \right)_{nl} + \Psi_{A,12} + \left(\frac{\langle L(\mathbf{n})R^*(\mathbf{0}) \rangle}{\langle R(\mathbf{n})R^*(\mathbf{0}) \rangle} \right)_{nl} + \Psi_{A,21} \right].$$

Note that the reference antenna is observing on-axis, so it has no leakage. The uncertainty in l_{QA} comes from the noise in the receivers:

$$|\sigma_{l_{QA}}|^2 = \sum_{S=RR^*,LL^*,RL^*,LR^*} \left| \frac{\partial l_{QA}}{\partial S} \sigma_S \right|^2$$

The source is intrinsically unpolarized, so the crosscorrelations without leakage, $\langle RL^* \rangle_{nl}$ and $\langle LR^* \rangle_{nl}$, are zero, and thus so are the derivatives of l_{QA} with respect to RR^* and LL^* . The

uncertainty of l_{QA} reduces to

$$|\sigma_{l_{QA}}(\mathbf{n})| = \frac{2\sigma_Q}{\langle L(\mathbf{n})L^*(\mathbf{0}) \rangle + \langle R(\mathbf{n})R^*(\mathbf{0}) \rangle}$$

$$= \frac{\sigma_Q}{|g_{\text{off-axis},A}(\mathbf{n})|I(\mathbf{0})}$$

since antenna A is the off-axis one. $\sigma_{l_{UA}}$ has the same form, and in our case is identical since $\sigma_Q = \sigma_U$.

The uncertainties are roughly independent of \mathbf{n} because of the time weighting, with an average value for antennas 2 to 6 of 0.0012. The beam centers are an exception, with average uncertainties for antennas 2 to 6 of 6×10^{-4} . Antennas 1 and 7 were each used as reference antennas half of the time, so their uncertainties are worse by a factor of nearly $\sqrt{2}$ (ameliorated by their slightly larger diameters).

7. DISCUSSION

The measured leakage patterns, Figs. 6 to 9, show that although there is some overall consistency in the patterns, their details are unpredictable, both from antenna to antenna and from band to band in frequency. Most noticeably, the antennas with quadrupod receiver supports, 1 and 7, are structurally nearly identical, but their leakage patterns do not show any more similarity to each other than they do to those of the tripod antennas. Likely this is because most of the leakage comes not from the struts, but from the feeds. The feeds are nominally identical, and their individual flaws are neither easily apparent to visual inspection nor tied to the type of antenna they are mounted on. This suggests that wide-field polarimetry with even nominally homogeneous arrays requires measuring the leakage patterns of each antenna, if the needed fidelity warrants it.

Variation of the leakage patterns from band to band is prominent in the real parts of the leakage patterns. This rapid change with frequency seems surprising at first glance: one might expect properties of a waveguide feed to vary quite slowly with frequency, and hardly at all across a band that is only 2% of the center frequency. The cause appears to be the probes used to feed the reflector at 408 MHz; they are housed within the 1420 MHz feed (Veidt et al. 1985). Computed simulations (B.G. Veidt, private communication) indicate that these probes cause some fine structure in the performance at 1420 MHz.

The primary voltage patterns, Figs. 10 and 11, reassuringly exhibit only the expected dependence on wavelength; namely their angular scales are proportional to the observing wavelength. Their apparent tight link to antenna structure suggests that primary voltage pattern errors are more amenable to correction by adjusting the antennas, as is often done using holograms. Once the primary voltage patterns are known, their effect can also be reduced post-observation, even for an inhomogeneous array (Bhatnagar et al. 2006). Currently such errors are attacked with direction dependent self-calibration (modcal, (Willis 1999), also called peeling), which is vulnerable to confusing true features on the sky with unwanted artifacts. Measuring the antenna patterns with a bright unresolved calibration source instead of through self-calibration with a potentially complicated fainter science target removes that vulnerability.

Although we have only tested heterogeneous array leakage correction with equatorially mounted antennas, in principle it would be even easier to adapt it to antennas on altitude-azimuth mounts than the image-based leakage map

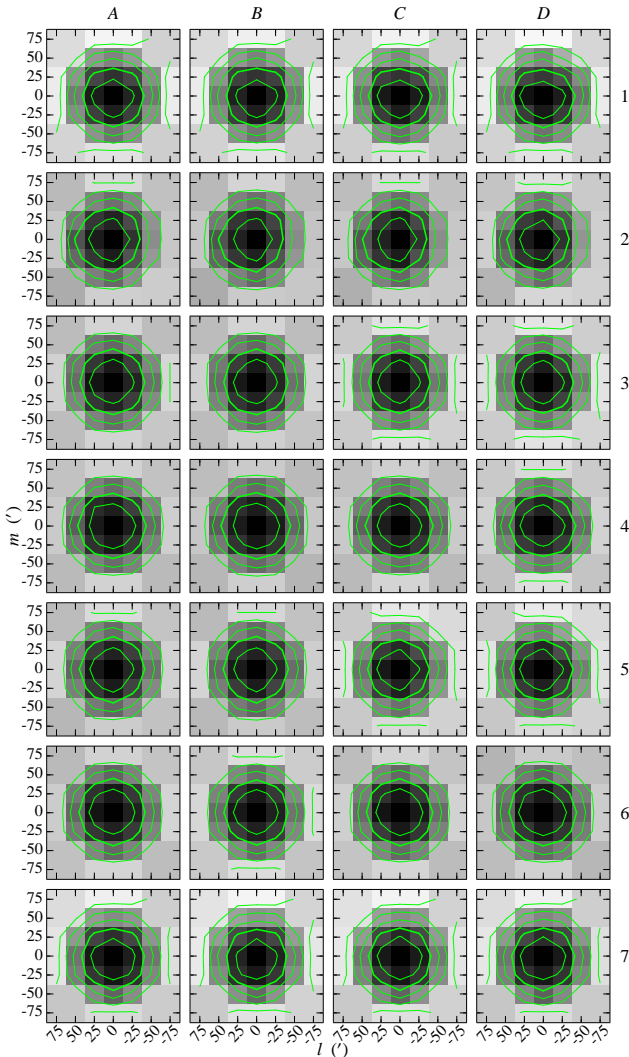


FIG. 10.— Real parts of the primary voltage patterns of antennas 1 (top) to 7 (bottom) for bands A (left) to D (right). The grayscale goes from 0.4 (white) to 1.0 (black), and the contours go from 0.4 to 0.9 in steps of 0.1.

method. Since the leakage voltage pattern method already deals with visibilities on an individual basis, the only modification needed would be make x_j and y_j in Equation 2 functions of time to account for the rotation of the antennas about the optical axis relative to the sky as the Earth turns.

An implicit, but difficult to avoid, assumption in correcting for the effect of beam patterns is that the patterns do not change with time or observing elevation. The prospect of spending observing time on frequent antenna pattern re-measurements, possibly for a set of elevations and frequencies, is unappealing, so there is considerable pressure to engineer antennas that are stable enough for occasional measurements to capture most of the effects. The ST antennas were not expected to change significantly with time or observing direction, but we confirmed their behavior by comparing recent leakage measurements to the measurements made by Peracaula of the ST’s overall leakage amplitude maps at 21 cm wavelength. There was little change over the intervening 10 years, despite some surface modifications to a few of the antennas. Stability is expected to be a more serious problem for larger (as measured in wavelengths) dishes, especially if standing waves create a noticeable resonance effect

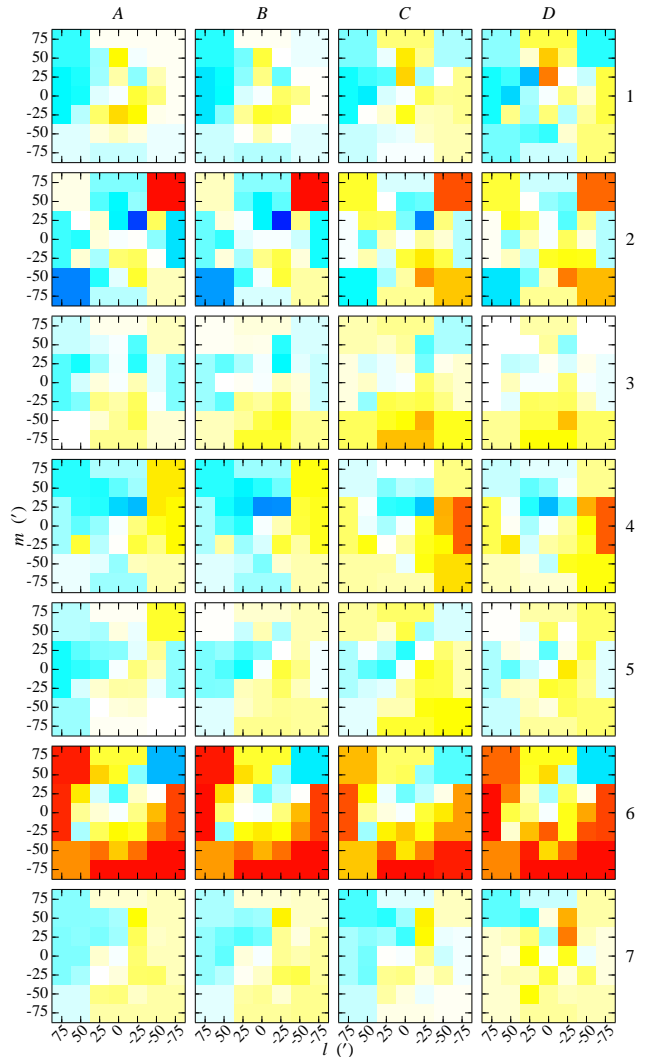


FIG. 11.— Imaginary parts of the primary voltage patterns of antennas 1 (top) to 7 (bottom) for bands A (left) to D (right). The colorscale goes from -0.1 (blue) to 0.1 (red). The symmetry of antenna 6’s patterns suggests that it is out of focus.

in the leakage at certain observing frequencies. Interpolation, or theoretical modeling, may be useful for extending the applicability of measured maps to additional elevations and/or frequencies. Alternatively, if an extremely accurate correction is only needed for one bright source within the field of an observation, the antenna patterns could be measured at that spot immediately before and after the science observation, as opposed to mapping the entire main lobe of the antenna patterns.

The National Radio Astronomy Observatory is a facility of the National Science Foundation operated under cooperative agreement by Associated Universities, Incorporated. The Dominion Radio Astrophysical Observatory is operated as a national facility by the National Research Council of Canada. The Canadian Galactic Plane Survey is a Canadian project with international partners. The survey is supported by a grant from the Natural Sciences and Engineering Council (NSERC). We thank the reviewers for their time and helpful comments.

R. Kothes kindly pointed out IC443 as a good example of the new correction method’s efficacy, and D. Routledge help-

fully expanded upon the simulations of Ng et al. We appreciate the assistance of J.E. Sheehan in facilitating the measurements and D. Del Rizzo in partially processing the data. The processing was also assisted by K. Douglas' program-

ming and documentation for antenna surface measurements. R.R. appreciates J. Uson, W. Cotton, C. Brogan, and D. Balser sharing their experience with the VLA and GBT.

REFERENCES

- Bhatnagar, S., Cornwell, T., & Golap, K. 2006, Correction of errors due to antenna power patterns during imaging, EVLA Memo 100, National Radio Astrophysical Observatory [1](#), [7](#)
- Bock, D. C.-J. 2006, in Astronomical Society of the Pacific Conference Series, Vol. 356, Revealing the Molecular Universe: One Antenna is Never Enough, ed. D. C. Backer, J. M. Moran, & J. L. Turner, 17–+, [ADS link 1](#)
- Clark, B. G. 1999, in ASP Conf. Ser. 180: Synthesis Imaging in Radio Astronomy II, ed. G. B. Taylor, C. L. Carilli, & R. A. Perley, 1–, [ADS link 1](#)
- Cotton, W. 1994, Widefield Polarization Correction of VLA Snapshot Images at 1.4 GHz, AIPS Memo 86, National Radio Astrophysical Observatory [1](#)
- Ekers, R. D. 1999, in ASP Conf. Ser. 180: Synthesis Imaging in Radio Astronomy II, ed. G. B. Taylor, C. L. Carilli, & R. A. Perley, 321–334, [ADS link 1](#)
- Högbom, J. A. 1974, A&AS, 15, 417, [ADS link 2](#)
- Hamaker, J. P., Bregman, J. D., & Sault, R. J. 1996, A&AS, 117, 137, [ADS link 1](#), [4](#)
- Heiles, C., Robishaw, T., Troland, T., & Roshi, D. A. 2003, [A Preliminary Report: Calibrating the GBT at L, C, and X Bands](#), GBT Commissioning Memo 23, NRAO [4](#)
- Landecker, T. L., Dewdney, P. E., Burgess, T. A., Gray, A. D., Higgs, L. A., Hoffmann, A. P., Hovey, G. J., Karpa, D. R., Lacey, J. D., Prowse, N., Purton, C. R., Roger, R. S., Willis, A. G., Wyslouzil, W., Routledge, D., & Vaneldik, J. F. 2000, A&AS, 145, 509, [ADS link 1](#)
- Ng, T., Landecker, T. L., Cazzolato, F., Routledge, D., Gray, A. D., Reid, R. I., & Veidt, B. G. 2005, Radio Science, 40, 5014 [3](#), [3](#)
- Peracaula, M. 1999, Instrumental polarization corrections at 1420 MHz for the DRAO Synthesis Telescope fields, Tech. rep., Dominion Radio Astrophysical Observatory [1](#)
- Sault, R. J. & Ehle, M. 1996, [The ATCA 13-cm Polarimetric Response](#), ATNF Technical Memo 39.3/088, CSIRO [4](#)
- Taylor, A. R., Gibson, S. J., Peracaula, M., Martin, P. G., Landecker, T. L., Brunt, C. M., Dewdney, P. E., Dougherty, S. M., Gray, A. D., Higgs, L. A., Kerton, C. R., Knee, L. B. G., Kothes, R., Purton, C. R., Uyaniker, B., Wallace, B. J., Willis, A. G., & Durand, D. 2003, AJ, 125, 1350 [1](#), [3](#)
- Thompson, A. R. 1999, in ASP Conf. Ser. 180: Synthesis Imaging in Radio Astronomy II, ed. G. B. Taylor, C. L. Carilli, & R. A. Perley, 11–, [ADS link 1](#)
- Veidt, B. G., Landecker, T. L., Dewdney, P. E., Vaneldik, J. F., & Routledge, D. 1985, Radio Science, 20, 1118, [ADS link 7](#)
- Willis, A. G. 1999, A&AS, 136, 603, [ADS link 7](#)